JOURNAL OF THERMOPHYSICS AND HEAT TRANSFER
Vol. 8, No. 3, July–Sept. 1994

Fluid Flow and Heat Transfer of an Extended Slot Jet Impingement

Y. J. Chou* and Y. H. Hung†
National Tsing Hua University, Hsinchu, Taiwan 30043, Republic of China

A numerical analysis for fluid flow and heat transfer of a confined slot jet impingement with an extended nozzle is performed. The parametric effects of jet Reynolds number, spacing between the confinement plate and the target surface, and nozzle length on local flow development and heat transfer characteristics of the heated target surface are explored. The viscous boundary-layer thickness at the stagnation line is presented. It may be well predicted by the correlation of a two-dimensional stagnation flow if the lateral velocity gradient just outside the viscous boundary layer is known. This lateral velocity gradient is linearly proportional to jet Reynolds number, while inversely proportional to the ratio of nozzle exit-to-target surface distance to nozzle width in a 0.34 power. In addition, new correlations for stagnation and local Nusselt numbers along the heated target surface are reported in this article. These correlations give satisfactory agreements with theoretical results.

Nomenclature

C = lateral velocity gradient just outside the viscous boundary layer for two-dimensional stagnation flow
d = nozzle length
H = confinement plate-to-target surface spacing
h_s = heat transfer coefficient at stagnation line
h_x = local heat transfer coefficient
L = half-length of target surface
Nu_s = Nusselt number at stagnation line, $h_s W/\kappa$
Nu_x = local Nusselt number, $h_x W/\kappa$
P = dimensionless pressure, $pW^2/\rho\nu^2$
Pr = Prandtl number, ν/α
p = fluid pressure
p_0 = ambient pressure
q''_x = local heat flux
Re_w = jet Reynolds number, $\bar{v}_j W/\nu$
S^ψ = source term of Eq. (2)
T = temperature
T_j = fluid temperature at nozzle inlet
T_w = temperature on the target surface
t = time
U = dimensionless velocity component parallel to the target surface, uW/ν
u = velocity component parallel to the target surface
V = dimensionless velocity component normal to the target surface, vW/ν
v = velocity component normal to the target surface
v_c = centerline velocity component normal to the target surface
$\bar{v}_j$ = average velocity at nozzle inlet
W = nozzle width
X^* = value of X where $(P - P_0)/(\frac{1}{2}\bar{V}_j^2) = 0$
X, Y = dimensionless coordinate, x/W, y/W
$X_{1/2}$ = half-width of the jet in jet flow development
x, y = coordinates shown in Fig. 1
α = thermal diffusivity of fluid
β = lateral velocity gradient along the jet centerline, defined in Eq. (12)
Γ^* = dimensionless diffusivity coefficients listed in Table 1
δ = viscous boundary-layer thickness
θ = normalized temperature, $(T - T_j)/(T_w - T_j)$
κ = thermal conductivity of fluid
ν = kinematic viscosity of fluid
ρ = density of fluid
τ = dimensionless time, $\nu t/W^2$
ϕ = transported scalar property

Subscripts
c = at centerline
j = at nozzle inlet
max = maximum value
s = at stagnation line
w = on target surface

Superscript
$-$ = average

Introduction

THE demand for compactness and higher operational speeds leads to high-power density in electronic packages. Improvement in cooling methods are required to avoid unacceptable temperature rise. An effective cooling technique of jet impingement with low air velocity, to meet the limitation of the resulting force of air jet exerted on the packages, is a promising way to achieve high thermal performance for compact multichip packages. The low turbulence jet with low velocity is sometimes referred to as "laminar" jet, since nozzle designs are employed which reduce turbulence.[1]

Two kinds of jet configuration, circular and slot jets, are employed in the existing study. From the survey of existing literature, it is found that one drawback in using a single circular jet is the concentration of cooling in the small impingement zone of the heated surface. Thus, the use of multiple jets enhances cooling uniformity by creating several impingement zones which cover a significant fracture of the heated surface. Nevertheless, multiple jets create flow blockage between the jets and complicate fluid distribution downstream from the impingement zone. These problems become extremely critical in the cooling of multichip packages, which requires uniform cooling of a large number of chips, ease of fluid introduction into, and smallest possible volume of fluid rejection from the module. To overcome the above problems, Wadsworth and Mudawar[2] performed an experimental cooling study for a simulated multichip module by means of a

Received March 15, 1993; revision received Sept. 1, 1993; accepted for publication Sept. 10, 1993.

*Graduate Student, Department of Power Mechanical Engineering.
†Professor, Department of Power Mechanical Engineering.

confined two-dimensional slot jet. They found that a potential solution to these problems was to use a two-dimensional slot jet which provided a larger impingement zone and insured uniform coolant rejection following impingement. In addition, cooling by means of a two-dimensional slot jet maintained nearly isothermal chip surface conditions. Therefore, a two-dimensional slot or planar jet offers some benefits such as cooling effectiveness, uniformity, and controllability on compact multichip packages.

Two-dimensional steady laminar boundary-layer equations for flow over a wedge having a constant surface temperature were solved.[3] A similarity solution is applicable to stagnation flow when the wedge angle equals 180 deg. The expression for viscous boundary-layer thickness, which was identical to that calculated from the Navier-Stokes equations,[4] indicated that boundary-layer analyses were appropriate to stagnation flows. Similarly, for other configurations such as a sphere, cylinder, and disc, the stagnation point heat transfer results were obtained.[5] From the results, the Nusselt number at the stagnation point of a body of revolution in a uniform flow depends on $Re^{0.5}$. This same dependency had been derived by Sparrow and Lee[6] for a nonuniform impinging slot jet. At the same time, Sparrow and Wong[7] used a naphthalene sublimation technique to measure the mass transfer coefficients of an air impinging jet on the naphthalene plate. With a heat-mass transfer analogy, the heat transfer coefficients could be obtained. They found that the transfer coefficients generally tended to decrease with increasing separation spacing. Increases in Reynolds number tended to increase the transfer coefficients. The surface distributions of the transfer coefficient were bell-shaped, with the largest value at the stagnation point. The stagnation point values were correlated with a 0.6-power dependence. Their experimental data were confirmed by the results of van Heiningen et al.[8] for a slot jet with a parabolic velocity profile. van Heiningen et al. explored the flowfield and heat transfer from a laminar impinging slot by solving the full Navier-Stokes equations with the appropriate boundary conditions. They numerically investigated a semi-confined laminar impinging slot jet with the stream-vorticity scheme. They found that Nu was proportional to $Re_w^{0.49}$ for a uniform velocity profile; while Nu was proportional to $Re_w^{0.6}$ for a parabolic velocity profile. Later, Masliyah and Nguyen[9] used another mass transfer technique, swollen polymer method, with a holographic technique to measure the recession of their sample under the same conditions. A simple correlation for the local Sherwood number under laminar conditions in the vicinity of the stagnation points was obtained. In 1984, Law and Masliyah[10] numerically studied the flowfield of a two-dimensional confined laminar submerged jet impinging on a flat surface. The jet exit velocity profile in their study was assumed to be fully developed. They defined the thickness of the viscous boundary layer in the stagnation flow region as the distance from the impingement plate where the lateral velocity reaches 99% of U_{max}. This boundary-layer thickness, which was quite constant throughout the stagnation flow region, could be determined from the lateral velocity profiles in the stagnation flow region. However, no information related to heat transfer was reported in their study.

According to Polat et al.,[11] most of the results reported in existing literature emphasized the heat transfer characteristics of impinging jets without confinement. Information on laminar fluid flow and heat transfer characteristics for jet impingement with an extended nozzle in a confined space is scarce. The various factors affecting the stagnation and local heat transfer behaviors have not been systematically investigated. In order to obtain a further understanding on the topic, a series of numerical studies have been conducted. The main objectives of this study are to investigate the viscous boundary-layer thickness at the stagnation line for a confined slot jet impingement with an extended nozzle; to explore the effects of jet Reynolds number, confinement plate-to-target plate spacing, and the extended nozzle length on local jet flow and heat transfer characteristics in such a geometric configuration; to compare the present numerical fluid flow and heat transfer results with the existing theoretical and experimental data; and to propose new Nu correlations for predicting stagnation and local heat transfer characteristics.

Theoretical Formulation

The geometric configuration to simulate a confined chip package with an extended slot jet impingement is shown in Fig. 1. A two-dimensional, incompressible laminar forced convection is employed in this analysis. A Newtonian fluid with constant properties is assumed. Furthermore, the viscous dissipation and the compressibility effect in the energy equation are neglected. Let

$$X = \frac{x}{W}, \quad Y = \frac{y}{W}, \quad U = \frac{uW}{\nu}, \quad V = \frac{vW}{\nu}$$
$$P = \frac{pW^2}{\rho\nu^2}, \quad \tau = \frac{\nu t}{W^2}, \quad \theta = \frac{T - T_j}{T_w - T_j} \tag{1}$$

where x and y represent the coordinates parallel to and normal to the heated target surface, respectively. The fluid velocity components u and v are in the x and y directions, respectively. The slot jet width is W. Finally, T_j and T_w are the nozzle inlet temperature and the heated target surface temperature, respectively.

With the above-mentioned assumptions, the general expression of the governing equations can be written in dimensionless form as follows:

$$\frac{\partial\psi}{\partial\tau} + \frac{\partial(U\psi)}{\partial X} + \frac{\partial(V\psi)}{\partial Y} = \frac{\partial}{\partial X}\left(\Gamma^* \frac{\partial\psi}{\partial X}\right) + \frac{\partial}{\partial Y}\left(\Gamma^* \frac{\partial\psi}{\partial Y}\right) + S^\psi \tag{2}$$

where ψ represent dimensionless transported scalar properties. All the dimensionless coefficients and sources terms of Eq. (2) are defined in Table 1.

Since the present computational domain is symmetric, half of the configuration would be adequate to simulate the problem. The dimensional boundary conditions over all boundaries of the domain are shown in Fig. 1, and the corresponding dimensionless boundary conditions are briefly described in the following paragraphs.

Fluid temperature at the nozzle inlet is taken to be uniform, i.e., $\theta = 0$. The fluid velocity profile at the nozzle inlet ($0 \leq$

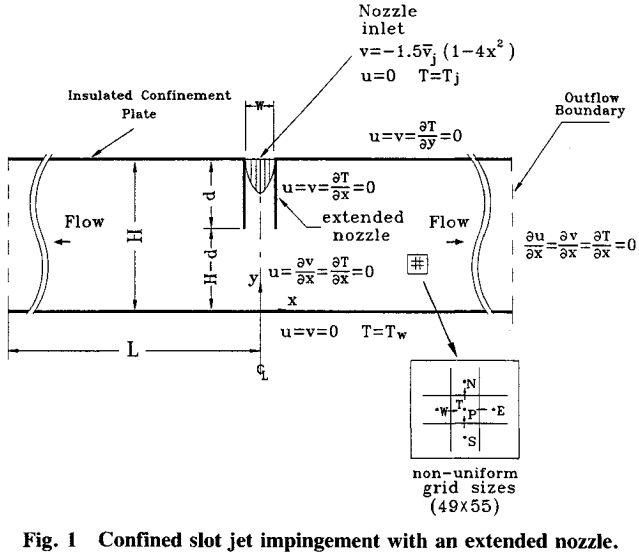

Fig. 1 Confined slot jet impingement with an extended nozzle.

Table 1 Dimensionless coefficients and source terms in Eq. (2)

Equation	ψ	Γ^*	S^ψ
Continuity	1	0	0
X Momentum	U	1	$-\frac{\partial P}{\partial X}$
Y Momentum	V	1	$-\frac{\partial P}{\partial Y}$
Energy	θ	$1/Pr$	0

$X \leq 0.5$, $Y = H/W$) is assumed as fully developed, i.e., the profile is parabolic and its expression is

$$U = 0, \qquad V = -1.5Re_w(1 - 4X^2) \tag{3}$$

No-slip, no suction/blowing conditions and zero temperature gradient are used at the insulated confinement surface ($X > 0.5$, $Y = H/W$), and at the extended nozzle surface ($X = 0.5$, $(H - d)/W \leq Y \leq H/W$). The conditions of transported properties are assumed to be invariant in the flow direction at the outflow boundary ($X = L/W$, $0 < Y < H/W$). Besides, no-slip, no suction/blowing and isothermal conditions are imposed at the heated target surface ($0 \leq X \leq L/W$, $Y = 0$), i.e., $U = V = 0$, $\theta = 1$. At the axis of symmetry ($X = 0$, $0 < Y < H/W$), the U velocity is set to 0, and the gradients of all other variables are set to 0.

Numerical Method

As we know, there are two methods, which are the iterative (with underrelaxation) and the time-marching procedures, for calculating steady-state solutions. In the present study, the time-marching method is employed. When time $t = 0$, all the solid surfaces and fluid are initially kept at the nozzle inlet temperature T_j. When time $t > 0$, only the target plate is heated with an isothermal condition.

In the present analysis, the governing equations can be integrated over the control volume and then discretized by using the power-law scheme with staggered grids.[12] Therefore, the final discretization equation can now be written as

$$A_P\psi_P = A_N\psi_N + A_S\psi_S + A_E\psi_E + A_W\psi_W + S^\psi$$
$$= \Sigma A_j\psi_j + S^\psi \quad (j = \text{N, S, E, or W}) \tag{4}$$

where ψ and j represent the local scalar quantity (U, V, P, or T), and the location of grid node (N, S, W, and E). S^ψ is the discretized source term.

Equation (4) is an interlinked algebra system because the coefficients of A_j are dependent on the scalar quantities ψ themselves. Thus, a semi-implicit iterative method, SIMPLEC, presented by van Doormaal and Raithby,[13] is implemented for steady-state solution in the present study.

The convergence criteria of the analysis are specified to meet the following conditions:

1) The maximum relative deviations of each local scalar quantity (U, V, P, or T) between successive iterations in the computational domain must be less than a small value, e.g., 10^{-4} in the present analysis.

2) The summation of the absolute residual of the mass conservation in each control cell is less than a small chosen value, e.g., 0.1% of total mass entering the flowfield.

Once the flowfield is obtained, the thermal field can then be solved. Therefore, the local heat transfer coefficient and Nusselt number can be evaluated, respectively, with the following equations:

$$h_x = \frac{q''_x}{T_w - T_j} = \frac{-\kappa\left(\frac{\partial T}{\partial y}\right)_{x,y=0}}{T_w - T_j} \tag{5}$$

$$Nu_x = \frac{h_x W}{\kappa} = -\frac{\partial\theta}{\partial Y}\bigg|_{X,Y=0} \tag{6}$$

From a numerical test, the vertical dimensionless displacement to exhibit invariant wall shear stress and heat flux transport from the wall is found when $\Delta Y \leq 0.01$. To keep a one-way boundary condition,[12] two numerical tests for exploring the effects of the target-surface length and grid size on the computational accuracy were conducted in the study. First, three different target-surface lengths, $L/W = 5$, 10, and 40, were tested. Compared with local distribution of Nusselt number for the case with $L/W = 40$, the maximum deviation of the local Nusselt numbers for the case with $L/W = 10$ is less than 0.5% in the region of $0 \leq X \leq 10$. This manifests that the choice of $L/W = 10$ is reasonable for numerical accuracy and computational time saving. This conclusion is consistent with that reported by Law and Masliyah.[10] Secondly, in order to balance numerical accuracy with time consumption, the grid meshes are set as ΔY or $\Delta X = 0.01$ near the solid boundaries, and then expanded nonuniformly in both the Y and X directions. There are five sets of grid sizes—25 × 35, 30 × 41, 35 × 46, 49 × 55, and 50 × 85—tested in the present study. The results show that the local Nusselt numbers calculated with the 49 × 55 grid sizes have insignificant deviations from those predicted with the finest grid sizes of 50 × 85. The maximum relative deviation is less than 0.1%. Thus, the grid sizes of 49 lines in the X direction, and 55 lines in the Y direction, is chosen for all computations in the present analysis.

Results and Discussion

The parameters explored in the present study are Pr 0.7, Re_w between 100–400, ratios of separation distance to nozzle width H/W ranged from 1 to 8, and ratios of nozzle length to nozzle width d/W varied from 0 to 7.

Jet Velocity Profile at Nozzle Exit

As we know, the jet flow will deflect when the jet impacts on the target surface. Thus, the impinging jet velocity profile will be influenced due to the flow deflection. Although the fluid velocity profiles at nozzle inlet for all cases are assumed to be fully developed in the analysis, the velocity profiles at nozzle exit may vary due to the effect of flow deflection caused by the existence of the target surface. Under a specified H/W value, the effect of target surface on the velocity profile at nozzle exit increases with increasing d/W ratio. Additionally, it is found that the velocity profile will be more easily influenced when the jet Reynolds number becomes smaller, e.g., $Re_w = 100$ in the study.

Half-Width Variations of Jet Flow in Flow Development

Several researchers have explored the growth of the jet in the flow development. The locus of the jet spreading is determined by the so-called "half-width of the jet flow," $X_{1/2}$. The half-width of the jet flow was defined as the distance between the centerline of the jet and a lateral point at which $v/v_c = 0.5$ at the same y elevation.[14,15]

Figure 2a exhibits the effect of jet Reynolds number on the half-width variation of the jet in the region of flow development for the cases of $H/W = 4$ and $d/W = 2$. For the case with a lower jet Reynolds number, e.g., $Re_w = 100$, the flow deflects earlier than for that with a higher jet Reynolds number, e.g., $Re_w = 400$. The normal distance of flow spreading

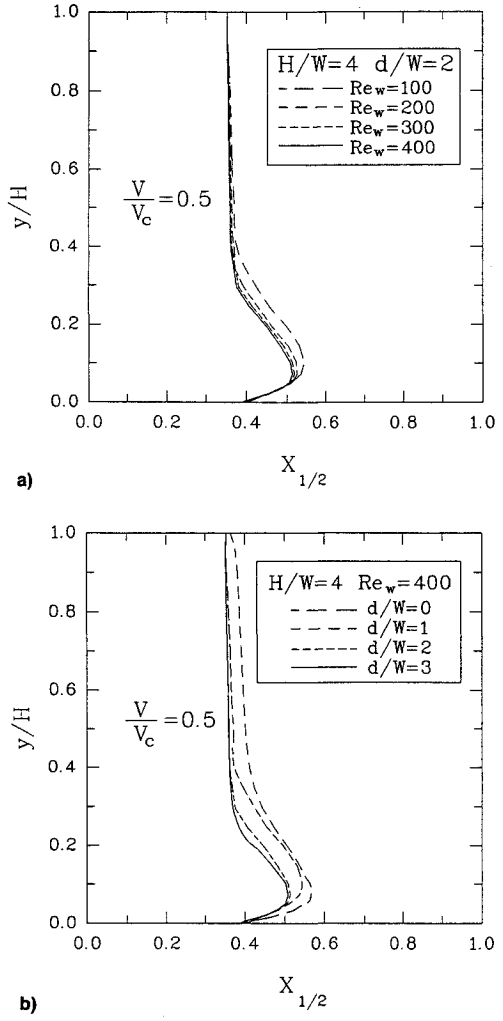

Fig. 2 Parametric effects on half-width of jet flow: a) effect of Re_w and b) effect of d/W.

with maximum lateral width y/H measured from the target surface, decreases with increasing jet Reynolds number, i.e., y/H = 0.1, 0.085, 0.082, and 0.080 for Re_w = 100, 200, 300, and 400, respectively. The maximum half-width of the jet decreases with increasing jet Reynolds number, i.e., $X_{1/2}$ = 0.55, 0.53, 0.52, and 0.51 for Re_w = 100, 200, 300 and 400, respectively.

The d/W effect on the half-width of the jet flow in the region of flow development is shown in Fig. 2b. The normal distance of jet spreading with maximum $X_{1/2}$ value measured from the target surface decreases with increasing d/W ratio, i.e., y/H = 0.1, 0.09, 0.080, and 0.078 for d/W = 0, 1, 2, and 3, respectively. The maximum half-widths of the jet flow are kept almost constant, i.e., $X_{1/2} \simeq 0.51$, when $d/W \geq 2$.

Variation of Lateral Velocity Gradient Along Jet Centerline

In two-dimensional impinging jet of finite width, some insight can be gained by considering analytical solutions for two-dimensional stagnation flow, which is a flow of infinite extent impinging normal to a surface. The viscous boundary-layer thickness for two-dimensional ideal stagnation flow reported by Schlichting[4] can be expressed as

$$\delta = 2.38(\nu/C)^{1/2} \tag{7}$$

The expression of Eq. (7) indicates that δ decreases with the magnitude of the velocity gradient C at the stagnation line. Values of C can be found from potential flow solutions of the freestream velocity field. Smaller jets or bluff bodies are characterized by higher values of the constant C because the fluid must be accelerated away from the stagnation line over shorter distances. Consequently, for real stagnation flows due to impinging jets of finite jet width without plate confinement, the constant C was experimentally found and expressed in the following form[16]:

$$C = (v_j/W)(1.02 - 0.024H/W), \qquad 1 \leq H/W \leq 10 \tag{8}$$

Consequently, the relative boundary-layer thickness δ/W is inversely proportional to the square root of the jet Reynolds numbers:

$$\delta/W = 2.38/[Re_w(1.02 - 0.024H/W)]^{1/2} \tag{9}$$

Furthermore, according to Zumbrunnen's results[17] for solving the integral equations of boundary layer of two-dimensional stagnation flow, δ and C at the stagnation line can be respectively expressed as

$$\delta = [(2/15)(C/\nu)]^{-1/2} \tag{10}$$

$$C = (\sqrt{3}/X^*)(\nu/W^2)Re_w \tag{11}$$

In Zumbrunnen's study, $X^* = 1.75$.

From the above studies, it is evident that the lateral velocity gradient near the stagnation line is of importance for determining the viscous boundary-layer thickness and other relevant transfer characteristics at the stagnation line. Therefore, it is valuable to explore the variation of lateral velocity gradient along the jet centerline (i.e., stagnation line). The lateral velocity gradient along the jet centerline in the present study of a confined slot jet with an extended nozzle is defined as

$$\beta = \left(\frac{\partial U}{\partial X}\right)_{X\to 0,Y} \tag{12}$$

However, in the present confined impinging-jet flows, it is very difficult to define a freestream velocity just beyond the boundary layer, as one used for two-dimensional stagnation flows or unconfined impinging-jet flows. To the authors' knowledge, the viscous boundary-layer thickness at the stagnation line for "confined" impinging-jet studies was defined only by Law and Masliyah[10] in existing literature. Law and Masliyah defined the thickness of the viscous boundary layer in the stagnation flow region as the distance from the impingement surface where the lateral velocity reaches 99% of U_{max}, the maximum value of velocity component in X direction for an individual profile of velocity component U. Therefore, based on Law and Masliyah's concept, a similar definition of viscous boundary-layer thickness at the stagnation line for the present study of confined jet impingement with an extended nozzle can be used. The boundary-layer thickness may be determined by the location of $Y = \delta/W$, where the value of U is maximum when $X \to 0$. This also represents that the β value is maximum at the edge of the defined boundary layer in the present study because of $U = 0$ at $X = 0$, i.e.,

$$\beta_{max} = \left(\frac{\partial U}{\partial X}\right)_{X\to 0,Y=\delta/W} \tag{13}$$

or

$$\left(\frac{\partial u}{\partial x}\right)_{x\to 0,y=\delta} = (\nu/W^2)\beta_{max} \tag{14}$$

The following explores the relevant parameters influencing the distribution of β and the defined boundary-layer thickness at the stagnation line.

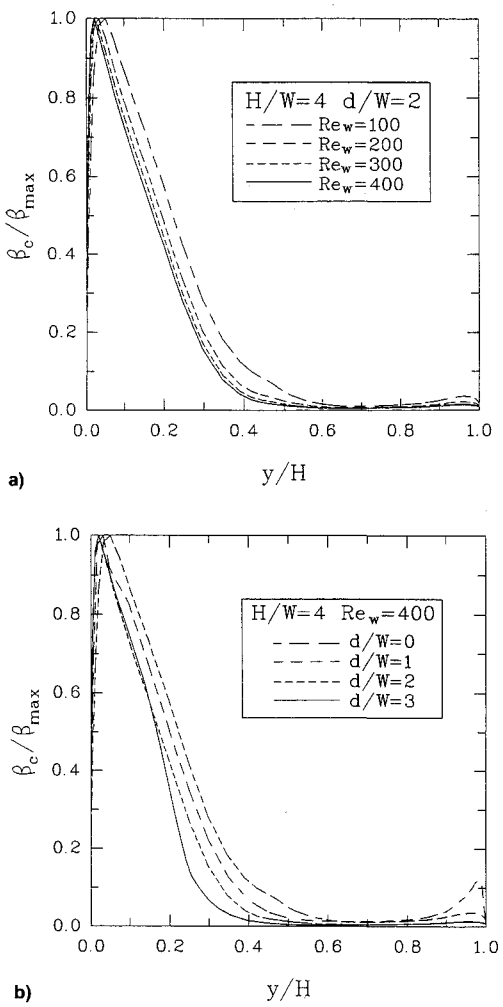

Fig. 3 Parametric effects on velocity gradient along jet centerline: a) effect of Re_w and b) effect of d/W.

The effect of jet Reynolds number on a normalized centerline velocity gradient β/β_{max}, for the cases of $H/W = 4$ and $d/W = 2$, is shown in Fig. 3a. From the figure, it displays that no significant lateral spread occurred in the abscissa until $y/H < 0.6$. The β_{max} values at the corresponding locations of boundary-layer edge are 169.10 at $\delta/H = 0.186$, 395.56 at $\delta/H = 0.129$, 638.63 at $\delta/H = 0.0952$, and 890.105 at $\delta/H = 0.0852$ for $Re_w = 100$, 200, 300, and 400, respectively. These results manifest that the β_{max} value at the stagnation line increases, while its corresponding boundary-layer thickness decreases, with increasing jet Reynolds number. Figure 3b shows the effect of d/W on β for cases of $Re_w = 400$ and $H/W = 4$. The local maximum values β_{max} with the corresponding locations are 716.09 at $\delta/H = 0.112$, 867.57 at $\delta/H = 0.090$, 890.11 at $\delta/H = 0.0852$, and 937.99 at $\delta/H = 0.0761$ for $d/W = 0$, 1, 2, and 3, respectively. The results manifest that the β_{max} increases, while δ/H decreases, with increasing d/W. It is obvious that at a higher d/W ratio, the jet fluid flow is more retarded and changes its direction earlier before impinging the target surface. Jet fluid flow at a larger d/W ratio is characterized by a higher value of β_{max}, since the fluid must be accelerated away from the stagnation line over shorter distances.

According to the above discussion of individual affecting parameters on the β distribution, it obviously evidences that the β_{max} distribution is the function of Re_w, H/W, and d/W. From the present numerical results, the relationship among β_{max}, Re_w, H/W, and d/W can be found in the following expression:

$$\beta_{max} = 2.55 Re_w[(H - d)/W]^{-0.34} \qquad (15)$$

From the analysis of all the data for cases of $H/W = 1$–8, $d/W = 0$–7, and $Re_w = 100$–400, the average relative deviation of the predictions using the above equations from the present numerical results shown in Fig. 4 is 8.10%. Besides, the numerical data for the laminar-confined slot jet cases with a parabolic jet exit velocity profile presented by Law and Masliyah[10] are shown in the figure for comparisons. The average relative deviation of the predictions using Eq. (15) from Law and Masliyah's data is 7.89%.

Moreover, the results evaluated with Eqs. (11) and (8), which represent two-dimensional stagnation flow[17] and unconfined slot jet flow,[16] respectively, are also presented in Fig. 4. A very essential conclusion may be drawn, i.e., all the data for the present confined slot jet impingement with an extended nozzle are higher than those for a unconfined slot jet with uniform profile in the ranges of $H/W = 1$–8, $d/W = 0$–7, and $Re_w = 100$–400.

Boundary-Layer Thickness at Stagnation Line

From Eqs. (7) and (10), it is obvious that the boundary-layer thickness for a two-dimensional stagnation flow is inversely proportional to $C^{0.5}$. In the present study for cases of

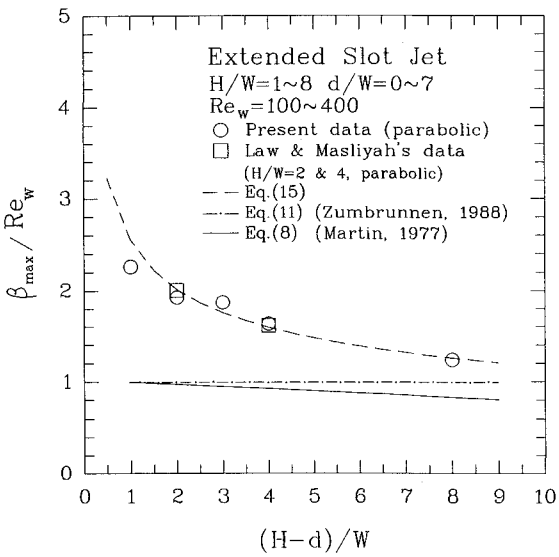

Fig. 4 Overall parametric effects on β_{max} distributions.

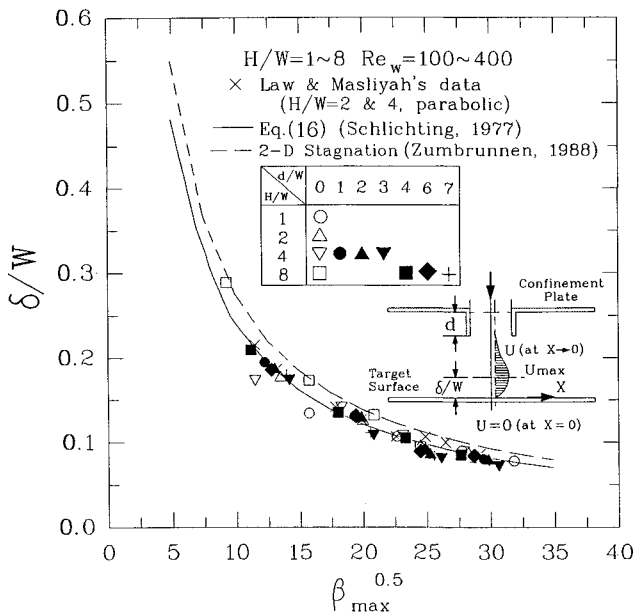

Fig. 5 Relationship between δ and β_{max}.

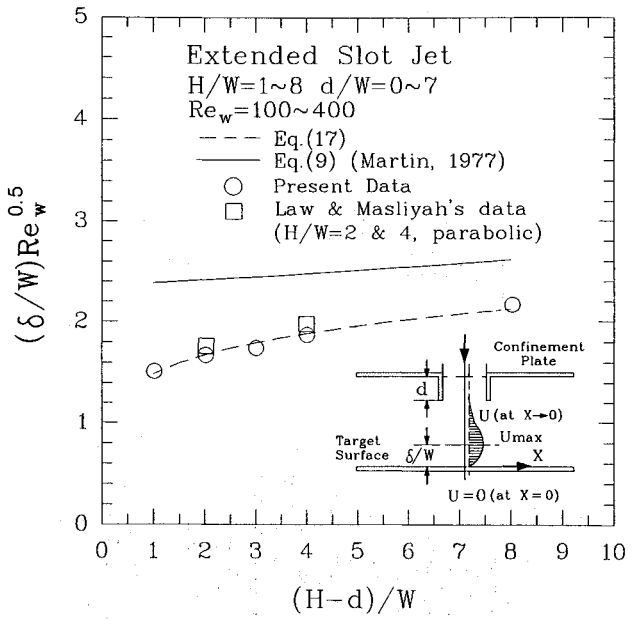

Fig. 6 Correlations of viscous boundary-layer thickness in terms of relevant parameters.

$H/W = 1$–8, $d/W = 0$–7, and $Re_w = 100$–400, the numerical results of δ/W vs $\beta_{max}^{0.5}$ are shown in Fig. 5. It is interesting to find that the present results will be very well predicted by the two-dimensional stagnation correlation in the ranges of parameters studied if $(\nu/W^2)\beta_{max}$ in Eq. (14) is used instead of C in Eq. (7), i.e.

$$\delta/W = 2.38\beta_{max}^{-0.5} \tag{16}$$

The average relative deviation of the present numerical results from the predictions using the above equation is 6.13% for all the cases of $H/W = 1$–8, $d/W = 0$–7, and $Re_w = 100$–400. For comparisons, the numerical data for the laminar confined slot jet cases with a parabolic jet exit velocity profile presented by Law and Masliyah[10] are also shown in the figure. The average relative deviation of Law and Masliyah's data from Eq. (16) is 5.52%.

Substituting Eq. (15) into Eq. (16), the viscous boundary-layer thickness at the stagnation line may be expressed in terms of relevant parameters as follows:

$$\delta/W = 1.49Re_w^{-0.5}[(H - d)/W]^{0.17} \tag{17}$$

Comparisons of Eq. (17) with the relevant results such as Law and Masliyah's data,[10] and Eq. (9) for an unconfined slot jet impingement,[16] are shown in Fig. 6. It is found that the δ/W values for the present confined slot jet impingement cases with an extended nozzle are usually smaller than those for unconfined slot jet cases.

Stagnation Heat Transfer

Relationship Between Nu_s and β_{max}

As discussed in the previous section, Re_w, ratio of nozzle exit-to-target surface distance to nozzle width, i.e., $(H - d)/W$, significantly influence the lateral velocity gradient near the stagnation line (i.e., β_{max}). For stagnation flow studies, the velocity gradient near the stagnation line determines the heat transfer performance at the stagnation line. For a two-dimensional stagnation flow, the heat transfer coefficient at the stagnation line reported by Kays and Crawford[18] can be expressed as

$$h_s = 0.57\kappa(C/\nu)^{0.5}Pr^{0.4} \tag{18}$$

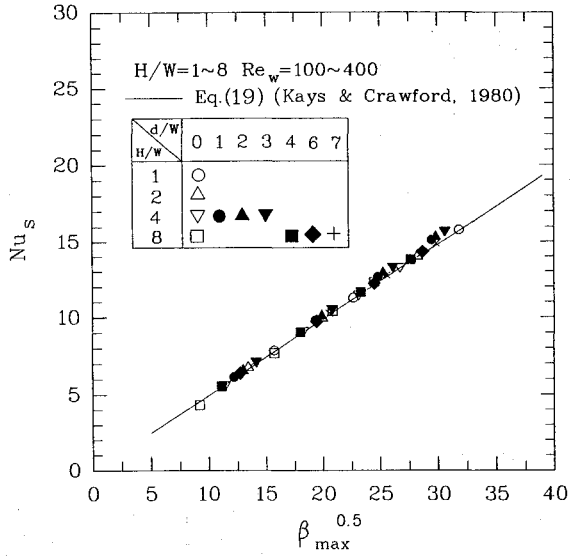

Fig. 7 Relationship between Nu_s and β_{max}.

In the present confined slot air jet impingement, $Pr = 0.7$, the C values in Eq. (18) may be considered as $(\nu/W^2)\beta_{max}$, so Eq. (18) becomes

$$Nu_s = 0.494\beta_{max}^{0.5} \tag{19}$$

Figure 7 shows the relationship between Nu_s and $\beta_{max}^{0.5}$ in the present study. Equation (19) is also plotted in the figure. It is interesting to note that the present results can be very well predicted with the two-dimensional stagnation correlation in Eq. (19). The maximum relative deviation of the present results and Eq. (19) is 1.51%. This manifests that the heat transfer characteristics at the stagnation line can be considered the same as that in a two-dimensional stagnation flow if β_{max} is known.

Nu_s Correlation in Terms of Relevant Parameters

Generally, Nu is proportional to $Re^{0.5}$ for many laminar jet impinging flows.[19] In the present confined jet impingement with an extended nozzle, the Nusselt number at the stagnation line, which is a local maximum value, can be correlated into the following two simple forms using Eq. (19) combined with Eqs. (16) and (15), respectively:

$$Nu_s = 1.176(\delta/W)^{-1} \tag{20}$$

$$Nu_s = 0.789Re_w^{0.5}[(H - d)/W]^{-0.17} \tag{21}$$

Equation (20) is exactly the same as that derived from the correlations for two-dimensional stagnation flow.[4,18] All the numerical data as well as the predictions using Eq. (21) are plotted in Fig. 8. From the results, it is notable that the average relative deviation between the present data and Eq. (21) is 5.09% with a maximum deviation of less than 15%. The range of parametric validity to use Eq. (21) is $7 \le Re_w^{0.5}[(H - d)/W]^{-0.17} \le 25$.

New Composite Nu_x Correlation

From the present results, the local Nusselt number in the wall jet region may be proposed to be composed of two limiting distributions, i.e., one is due to flow stagnation effect, and the other is due to downstream wall effect. Therefore, a bell-like distribution, representing the heat transfer characteristics in the vicinity of stagnation line, may be proposed as

$$(Nu_x)_s = Nu_s \exp(-0.05X^2) \tag{22}$$

All the numerical data are fitted by Eq. (22) with a maximum deviation of less than 5.5% in the region of $X \le 0.5$.

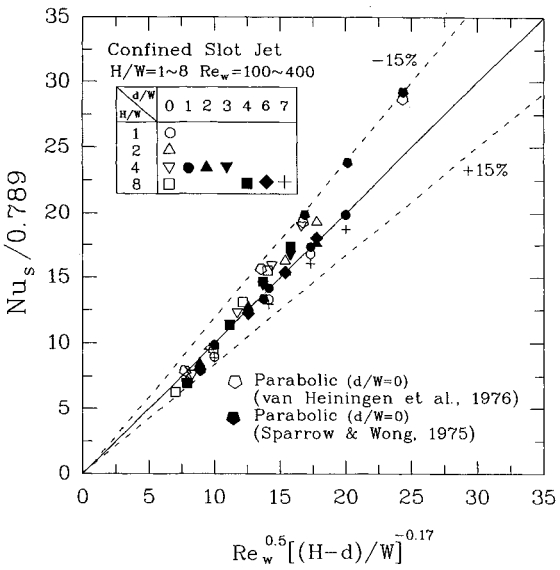

Fig. 8 Nu_s correlation in terms of relevant parameters.

In addition, to investigate the local Nusselt number in the wall jet region, the Pohlhausen's solution of local Nusselt number for a flat plate[18] is used to compare with the present results. The Pohlhausen's solution used in the present study can be expressed as

$$Nu_x = 0.332Pr^{1/3}(Re_w/X)^{1/2} \tag{23}$$

Considering the wall jet region affected by the impinging jet, a scaling position in the X direction, where the velocity component perpendicular to the target surface drops to its mean value, is proposed to effectively render the plot independent of the Pohlhausen's solutions for the parabolic velocity profile at nozzle inlet in the present study. The scaling positions S_x, evaluated from Eq. (3), are 0.29 for the parabolic velocity profile. Consequently, the modified Pohlhausen's solution, representing the characteristics in the downstream region, e.g., $X \geq 3.5$, for various Re_w, H/W, and d/W values in the present study ($Pr = 0.7$), can be expressed as

$$(Nu_x)_p = 0.295[Re_w/(X - S_x)]^{1/2}$$

$$X \geq 3.5 \tag{24}$$

Moreover, the present confined slot jet flow is similar to a boundary-layer growth on a flat surface, as the flow changes its direction and the main flow motion becomes transverse. Nevertheless, this is not true at the farther downstream location where the flow pattern becomes a developed channel flow. The modified Pohlhausen's solution may be considered to be valid for $3.5 \leq X \leq 10$ in the present study.

Using an approximate composite relation suggested by Churchill and Usagi,[20] a form to represent the Nu_x distribution in the wall jet region of confined slot jet flow may hereby be expressed as

$$Nu_x/Re_w^{0.5} = [(Nu_x/Re_w^{0.5})_s^n + (Nu_x/Re_w^{0.5})_p^n]^{1/n} \tag{25}$$

where $(Nu_x)_s$ and $(Nu_x)_p$ are expressed in Eqs. (22) and (24), respectively.

As fitted with the present numerical results in the region of $0 \leq X \leq 10$, the optimum value of n shown in Eq. (25) can be found as -5, i.e., Eq. (25) becomes

$$Nu_x/Re_w^{0.5} = [(Nu_x/Re_w^{0.5})_s^{-5} + (Nu_x/Re_w^{0.5})_p^{-5}]^{-1/5} \tag{26}$$

The local Nu_x distributions, as well as the predicted curves using Eq. (26) for cases of $H/W = 4$ under different Re_w and

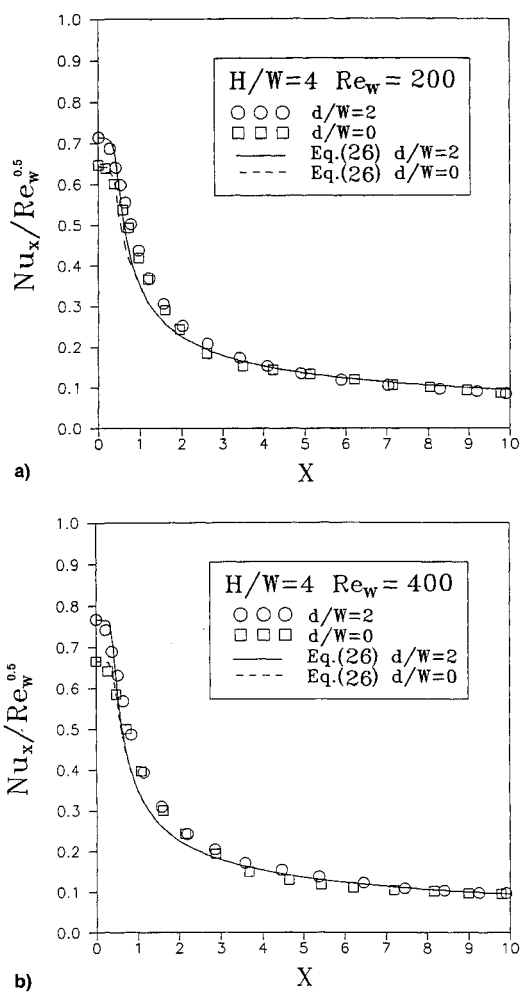

Fig. 9 Local Nusselt number distributions: a) Re_w = 200 and b) Re_w = 400.

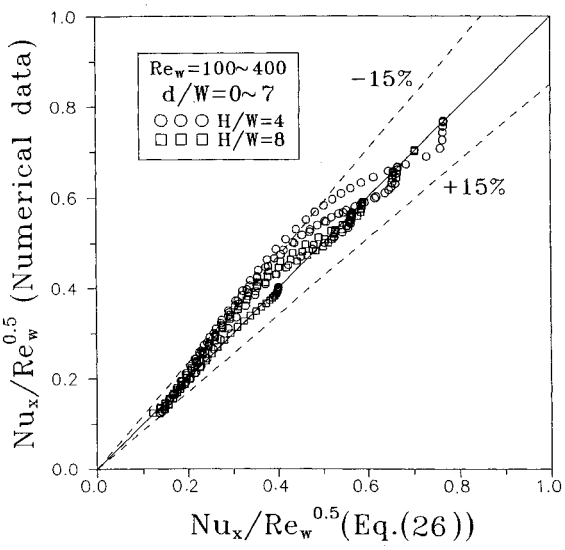

Fig. 10 Comparison of local Nusselt number between numerical results and Eq. (26).

d/W values, are presented with satisfactory agreements in Fig. 9. Furthermore, the comparisons between the predictions using Eq. (26) and the numerical data (235 points) for all the cases of H/W = 1–8, d/W = 0–7, and Re_w = 100–400 are made and plotted in Fig. 10. The average deviation between them is 7.84% with a maximum deviation less than 16.78%.

Concluding Remarks

A numerical investigation on fluid flow and heat transfer of a confined slot air jet impingement with an extended nozzle has been systematically performed in the study. The main conclusions emerging from the results and discussion may be summarized as follows:

1) A reasonable definition of viscous boundary-layer thickness at the stagnation line for a confined slot jet impingement with an extended nozzle is presented. In the parametric ranges of $H/W = 1-8$, $d/W = 0-7$, and $Re_w = 100-400$, the viscous boundary-layer thickness may be well predicted by the correlation of a two-dimensional stagnation flow if the velocity gradient just outside the viscous boundary layer is known.

2) The lateral velocity gradient just outside the viscous boundary layer is linearly proportional to the jet Reynolds number; however, it is inversely proportional to the nozzle exit-to-target surface distance in a 0.34 power.

3) The ratio of viscous boundary-layer thickness at the stagnation line to nozzle width is inversely proportional to the jet Reynolds number in a 0.5 power, while it is proportional to the nozzle exit-to-target surface distance in a 0.17 power.

4) The heat transfer characteristics at the stagnation line in the present configuration can be considered the same as that in a two-dimensional stagnation flow if the lateral velocity gradient just outside the viscous boundary layer is known.

5) A new correlation of Nusselt number at the stagnation line is proposed in terms of Re_w and $(H - d)/W$ for a confined slot jet impingement with an extended nozzle. The range of parametric validity to use this correlation is $7 \leq Re_w^{0.5}[(H - d)/W]^{-0.17} \leq 25$.

6) A new composite Nu_x correlation in the wall jet region is postulated. Comparisons between the present data and the predictions are made with a satisfactory agreement.

References

[1]Hoyt, J. W., and Taylor, J. J., "Effect of Nozzle Boundary Layer on Water Jets Discharging in Air," *Jets and Cavities—International Symposium*, American Society of Mechanical Engineers, New York, 1985, pp. 93–100.

[2]Wadsworth, D. C., and Mudawar, I., "Cooling of a Multichip Electronic Module by Means of Confined Two-Dimensional Jets of Dielectric Liquid," *Journal of Heat Transfer*, Vol. 112, Nov. 1990, pp. 891–898.

[3]Burmeister, L. C., *Convective Heat Transfer*, Wiley, New York, 1983, pp. 312–319, 384–393.

[4]Schlichting, H., *Boundary Layer Theory*, 7th ed., McGraw-Hill, New York, 1979.

[5]Van Der Meer, T. H., "Heat Transfer from Impinging Flame Jets," Ph.D. Dissertation, Technical Univ. of Delft, Delft, The Netherlands, Sept. 1987.

[6]Sparrow, E. M., and Lee, L., "Analysis of Flow Field and Impingement Heat and Mass Transfer Due to a Nonuniform Slot Jet," *Journal of Heat Transfer*, Vol. 97, May 1975, pp. 191–197.

[7]Sparrow, E. M., and Wong, T. C., "Impingement Transfer Coefficients Due to Initially Laminar Slot Jets," *International Journal of Heat and Mass Transfer*, Vol. 18, July 1975, pp. 597–605.

[8]Van Heiningen, A. R. P., Mujumdar, A. S., and Douglas, W. J. M., "Numerical Prediction of the Flow Field and Impingement Heat Transfer Caused by a Laminar Slot Jet," *Journal of Heat Transfer*, Vol. 98, Nov. 1976, pp. 654–658.

[9]Masliyah, J. H., and Nguyen, T. T., "Mass Transfer Due to an Impinging Slot Jet," *International Journal of Heat and Mass Transfer*, Vol. 22, Feb. 1979, pp. 237–244.

[10]Law, H. S., and Masliyah, J. H., "Numerical Prediction of the Flow Field Due to a Confined Laminar Two-Dimensional Submerged Jet," *Computers and Fluids*, Vol. 12, No. 3, 1984, pp. 199–215.

[11]Polat, S., Huang, B., Mujumdar, A. S., and Douglas, W. J. M., "Numerical Flow and Heat Transfer Under Impinging Jets: A Review," *Annual Review of Numerical Fluid Mechanics and Heat Transfer*, edited by C. L. Tien and T. C. Chawla, Vol. 2, Hemisphere, New York, 1989, pp. 157–197.

[12]Patankar, S. V., *Numerical Heat Transfer and Fluid Flow*, Hemisphere, New York, 1980.

[13]Van Doormaal, J. P., and Raithby, G. D., "Enhancement of the SIMPLE Method for Predicting Incompressible Fluid Flow," *Numerical Heat Transfer*, Vol. 7, No. 2, 1984, pp. 147–163.

[14]Womac, D. J., "Single Phase Axisymmetric Liquid Jet Impingement Cooling of Discrete Heat Sources," M.S. Thesis, School of Mechanical Engineering, Purdue Univ., West Lafayette, IN, 1989.

[15]Hsu, C. H., "Laser Doppler Anemometry Measurements of a Confined Turbulent Water Jet with a Uniform Background Flow," Ph.D. Dissertation, Virginia Polytechnic Inst. and State Univ., Blacksburg, VA, 1989.

[16]Martin, H., "Heat and Mass Transfer Between Impinging Gas Jets and Solid Surfaces," *Advances in Heat Transfer*, Vol. 13, Academic Press, New York, 1977, pp. 1–60.

[17]Zumbrunnen, D. A., "A Study of Heat Transfer from Stationary and Moving Plates Cooled by Planar Jets of Water," Ph.D. Dissertation, School of Mechanical Engineering, Purdue Univ., West Lafayette, IN, 1988.

[18]Kays, W. M., and Crawford, M. E., *Convective Heat and Mass Transfer*, 2nd ed., McGraw-Hill, New York, 1980.

[19]Downs, S. J., and James, E. H., "Jet Impingement Heat Transfer—A Literature Survey," American Society of Mechanical Engineers Paper 87-HT-35, Aug. 1987.

[20]Churchill, S. W., and Usagi, R., "A General Expression for the Correlation of Rates of Transfer and Other Phenomena," *AIChE Journal*, Vol. 18, No. 6, 1972, pp. 1121–1128.